

# Structure Functions and Low- $x$ Working Group Summary

Burkard Reiser<sup>1</sup>, Agustin Sabio Vera<sup>2</sup> and Zhiqing Zhang<sup>3</sup>

1- Max-Planck-Institut für Physik  
Föhringer Ring 6, 80805 München - Germany

2 - Instituto de Física Teórica UAM/CSIC,  
Universidad Autónoma de Madrid, E-28049 Madrid - Spain

3- Laboratoire de l'Accélérateur Linéaire  
Université Paris-Sud 11 et IN2P3/CNRS, Orsay - France

A summary of recent results reported in the Structure Functions and Low- $x$  working group at the DIS 2009 Workshop is given.

## 1 Introduction

Nucleon structure functions and their scale variations are closely related to the origins of Quantum Chromodynamics (QCD) as a gauge theory of the strong interaction. Precision data from HERA and the Tevatron lay the foundation of a quantitative understanding of the nucleon's structure in terms of parton distribution functions and their uncertainties.

## 2 Deep Inelastic Scattering

Since the completion of the HERA program at DESY considerable progress has been made to perfect the measurement of the inclusive electron/positron proton cross sections. An impressive amount of published and new preliminary neutral and charged current inclusive cross section and structure function data covering the entire HERA kinematic regime became available over the year passed since the DIS meeting in 2008.

### 2.1 Precision Measurements at Low and Medium- $Q^2$

A new measurement [2] of the inclusive positron proton cross section using approximately  $22 \text{ pb}^{-1}$  of data recorded by the H1 detector in 2000 was presented by Kretzschmar. The new measurement covers a range of medium four momentum transfer squared,  $12 < Q^2 < 150 \text{ GeV}^2$  and inelasticity  $y < 0.6$ . For the reconstruction of the kinematic variables, two methods are employed, one relying solely on the measurement of the scattered electron, the other also including information about the hadronic final state. For the final measurement, the reconstruction method which yields the smallest systematic uncertainty is used.

Petrukhin reported an extension of the H1 inclusive cross section measurements [3] towards low- $Q^2$ ,  $0.2 < Q^2 < 12 \text{ GeV}^2$ . This measurement is based on a dedicated shifted vertex run which improved the detector acceptance for low- $Q^2$  and a minimum bias run with open triggers for low- $Q^2$  inclusive data. Both runs were done in 1999 and 2000 during the HERA-I period.

The new H1 measurements at medium and low- $Q^2$ , are combined with the published H1 results [4] using an averaging procedure which takes into account correlated systematic uncertainties. The combination of the measurements not only yields smaller statistical errors but also a better understanding of the systematic uncertainties. The combination and reanalysis of the old data revealed a small,  $Q^2$ -dependent bias in the old data of up to 2.5%. After the combination an unprecedented accuracy of 1.3% to 2% is achieved.

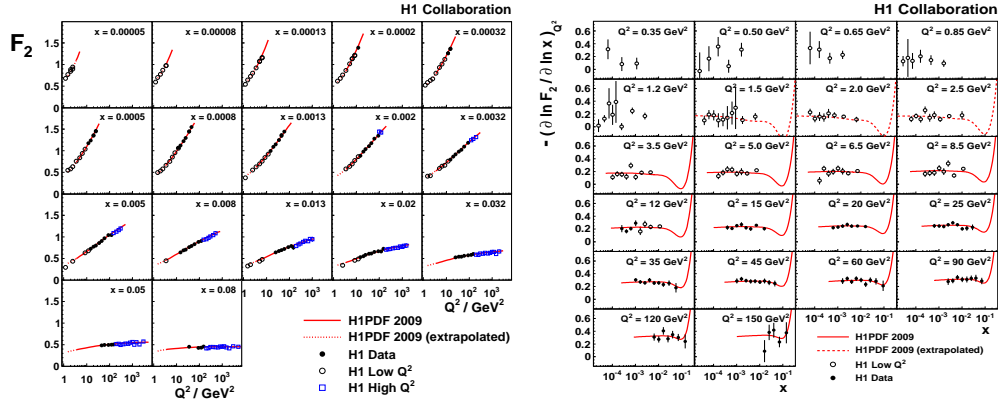


Figure 1: Measurement of the proton structure function  $F_2$  as a function of  $Q^2$  for fixed values of  $x$  (left) and of the derivative  $\partial \ln F_2 / \partial \ln x|_{Q^2}$  as a function of  $x$ .

The accurate measurements of the cross section allow for an extraction of the proton structure function  $F_2$  and its derivatives, as shown in Fig. 1. In the perturbative regime ( $Q^2 \geq \mathcal{O}(1 \text{ GeV}^2)$ ) the measurements are well described by NLO predictions. At lower  $Q^2$ , i.e. in the transition region towards non-perturbative QCD, phenomenological models (e.g. the colour dipole model[5, 6] or a fractal fit [7] based on the concept of self similarity) are found to give a decent parameterisation of the measurement. At low Bjorken  $x$ ,  $F_2$  can be parameterised as  $F_2 = c(Q^2)x^{-\lambda(Q^2)}$  allowing for an extrapolation of  $F_2$  towards even lower  $x$  i.e. higher  $y$  enabling an indirect determination of the structure function ratio  $R = F_L/(F_2 - F_L)$ . The value of averaged  $R$  for  $Q^2 < 12 \text{ GeV}^2$  extracted in this model dependent way is found to be consistent with  $R = 0.5$ , which is twice higher than that obtained from direct measurements of  $F_L$ , see the following section.

## 2.2 Direct Measurement of the Longitudinal Structure Function $F_L$

The reduced NC  $ep$  inclusive cross section is expressed in terms of structure functions by  $\sigma_r = F_2(x, Q^2) - y^2/Y_+ F_L(x, Q^2)$  with  $Y_+ = 1 + (1-y)^2$ . The structure functions  $F_2$  and  $F_L$  can be extracted from the measurement of  $\sigma_r$  at fixed  $x$  and  $Q^2$  but varying  $y$ . The kinematic variables  $x$ ,  $Q^2$  and  $y$  are related by  $y = \frac{Q^2}{x \cdot s}$  where  $s$  is the electron proton centre-of-mass energy squared. Therefore varying  $y$  – while keeping  $x$  and  $Q^2$  constant – requires to vary  $s$ . At HERA the variation of  $s$  was achieved by lowering the proton energy from 920 GeV to 460 GeV in the so-called low energy run, LER, and to 575 GeV for the medium energy run, MER. During a dedicated running period at the end of the HERA program both colliding beam experiments, H1 and ZEUS record approximately  $14 \text{ pb}^{-1}$  of LER and  $7 \text{ pb}^{-1}$  of MER data.

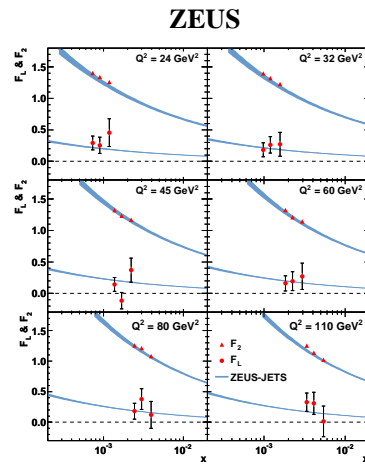


Figure 2: ZEUS  $F_L$  and  $F_2$  as a function of  $x$  at fixed  $Q^2$ .

Both H1 and ZEUS recently published first results of the longitudinal structure function  $F_L$  at medium  $Q^2$  [8, 9]. The ZEUS analysis, presented by Grebenyuk, combines the LER and MER with cross sections measured with approximately  $44\text{pb}^{-1}$  at the nominal centre-of-mass energy. The latter constitutes the most precise cross section measurement of ZEUS in the kinematic region covered. The extracted values of  $F_L$  and  $F_2$  displayed in Fig. 2 are well described by the NLO prediction based on the ZEUS-JETS fit. For the  $Q^2$  range covered, 24 to  $110\text{GeV}^2$ , ZEUS quotes a value of  $R = 0.18^{+0.07}_{-0.05}$ .

The H1 analysis, presented by Glazov, profited from the continued efforts to improve the backward calorimetry and tracking systems as well as from various trigger upgrades to enhance the trigger efficiency of low energy electrons. This enables H1 to measure the scattered electron at an energy as low as  $3\text{GeV}$ , while using the charge measurement of the track associated with the electron candidate to control the background. H1 have extended their published measurement towards high- $Q^2$ , up to  $800\text{GeV}^2$ , and low- $Q^2$ , down to  $2.5\text{GeV}^2$ , and obtain values of  $F_L$  at up to 6 different values of  $x$  at a given  $Q^2$ . The  $F_L$  averaged over  $x$  as a function of  $Q^2$  is shown in Fig. 3. For  $Q^2 > 10\text{GeV}^2$ , the measurement is well described by NLO predictions, whereas at lower  $Q^2$  the perturbative QCD calculation underestimates the measurement. Dipole models are found to describe the data well. For the entire  $Q^2$ -range the measurement is consistent with a value of  $R = 0.25$ .

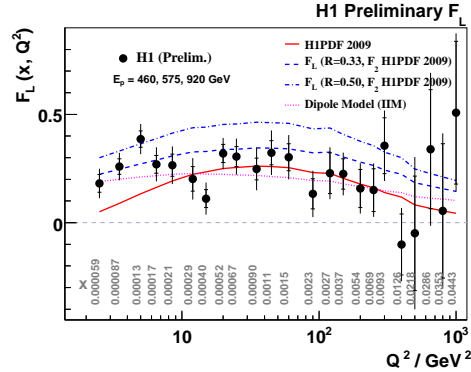


Figure 3: H1 average  $F_L$  as a function of  $Q^2$ .

### 2.3 Neutral and Charged Current Cross Sections at High- $Q^2$

New measurements by ZEUS of neutral (NC) and charged current (CC) cross sections at high- $Q^2$  were presented by Cooper-Sarkar. ZEUS recently published the measurement of NC [12] and CC [13]  $e^-p$  cross sections based on  $169\text{pb}^{-1}$  and  $175\text{pb}^{-1}$ . This new data samples are approximately 10 times larger than those of the previous publication from the HERA-I period. This enables a much improved measurement of the structure function  $x\tilde{F}_3$ , see Fig. 4. In addition preliminary measurements of the NC and CC  $e^+p$  cross sections were presented. Since the HERA upgrade the machine operated with polarised electron/positron beams. For both lepton beam charges, measurements with positive and negative polarisation are now available, and effects of the polarisation have been

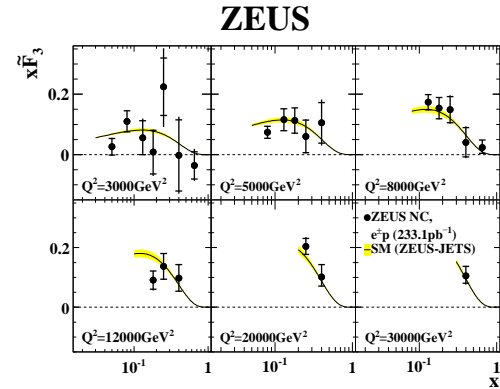


Figure 4: The structure function  $x\tilde{F}_3$  as a function of  $x$  at fixed  $Q^2$ .

clearly established both for CC and NC processes, giving striking confirmation of the Standard Model prediction for the chiral structure of the weak interactions.

## 2.4 Combined Cross Section of HERA-I

Tassi reported on the update of the combination of cross section measurements from H1 and ZEUS applying the averaging procedure presented at DIS 2008 [14]. In addition to the data already incorporated last year, the updated HERA combined cross section now also include the H1 low and medium  $Q^2$  cross sections (see above) and the low  $Q^2$  data recorded with the small angle ZEUS beam-pipe calorimeter (BPC [15]) and beam-pipe tracker (BPT [16]) as well as data from ZEUS recorded during a dedicated data taking period with shifted nominal vertex position [17] to increase the acceptance of small polar angles of the scattered electron. The ZEUS and H1 data are shifted to a common  $x$ - $Q^2$ -grid. Relying on the trivial assumption that both experiments are bound to measure the same cross section at the same  $x$  and  $Q^2$ , the averaging procedure not only reduces the statistical errors but also reduces the systematic uncertainty of the combined cross section. The global fitting groups expressed their great interest that the averaged HERA-I cross sections, which now comprise the complete set of the HERA-I inclusive measurements, are made available in order to be incorporated in the global fits.

## 2.5 Structure Function Measurements at HERMES

Gabbert reported on new measurements of the proton and deuteron structure functions  $F_2^p$  and  $F_2^d$  by the HERMES collaboration, which uses the HERA electron/positron beam in fixed target mode. The results are based on a data sample which is 10 (5) times larger than that of the proton (deuteron) structure function measurements by NMC with which this

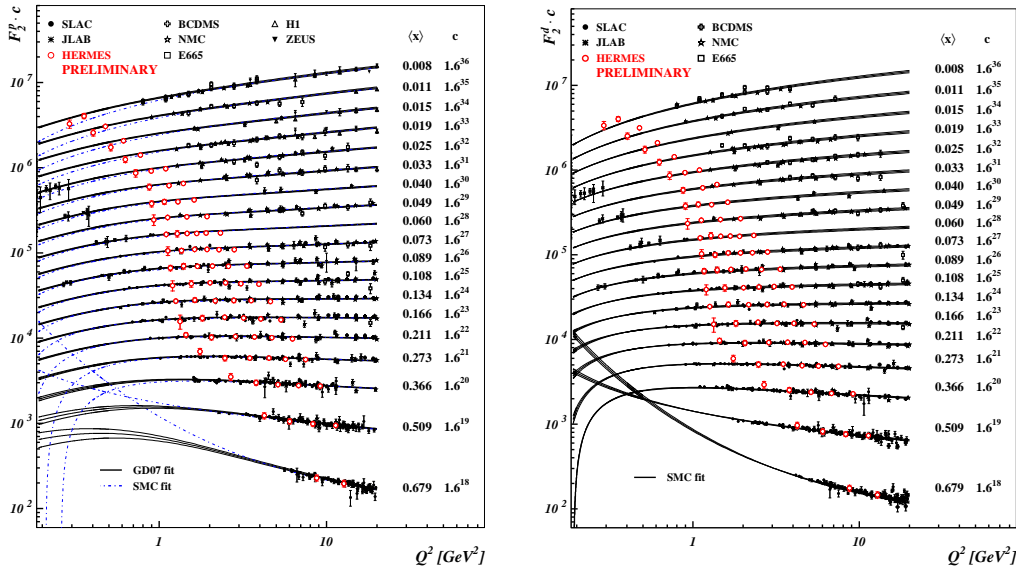


Figure 5: Measurement of the proton structure function  $F_2^p$  (left) and deuteron structure function  $F_2^d$  (right) by the HERMES collaboration.

new measurements overlap. The measurements are found to be consistent with previous measurements. Towards low  $x$  and  $Q^2$  the HERMES data explore a new kinematic region hitherto uncovered by experimental data. A new measurement of the cross section ratio  $\sigma^d/\sigma^p$  was obtained. It will be interesting to see the impact of this new data in future global fits, as well as its impact on extractions of the Gottfried Integral and the valance quark ratio ( $d_v/u_v$ ) at high  $x$ .

### 3 Proton Anti-Proton Collisions

Results from the Tevatron experiments, CDF and DØ, were presented by McNulty and Fox. The Tevatron  $p\bar{p}$  data provide important constraints for  $d_v$  and  $u_v$  valence quarks via the measurement of  $W$  and  $Z$  production and of the gluon distribution at high  $x$  via the measurement of inclusive jet cross sections. Recently both experiments invested quite some effort to extend their measurements to larger rapidities  $\eta$  thus simultaneously probing the high- and low- $x$  domain. The extension to high rapidities ( $\eta \sim 2$ ) at the Tevatron helps constraining standard model processes at the LHC at central rapidities ( $\eta = 0$ ).

#### 3.1 Inclusive Jet Cross Sections

Both experiments presented measurements of the double differential cross sections  $d^2\sigma/dp_T dy$  using  $0.7 \text{ fb}^{-1}$  for the DØ and  $1.13 \text{ fb}^{-1}$  for the CDF analysis. The measurements cover a  $p_T$ -range from 50 to 600 GeV and extend to a rapidity of 2.1 (CDF) and 2.4 (DØ). Within the systematics of the measurements the results of CDF [18, 19] and DØ [20] are in mutual agreement and are also well described by NLO QCD calculations. The impact of jet measurements on the gluon at high- $x$  has been studied in dedicated PDF fits by varying the jet datasets included in the fit, yielding variations of the gluon central value larger than the uncertainty bands obtained in the individual fits, examples of the resulting gluon are shown in Fig. 6. A detailed understanding of the gluon at high- $x$  requires further dedicated study.

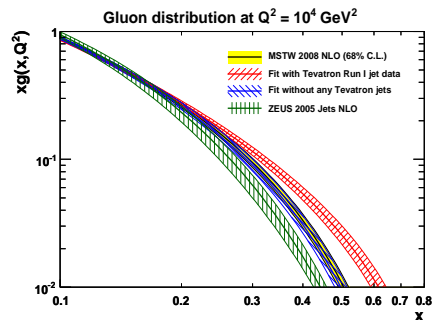


Figure 6: Comparison of high- $x$  gluons obtained from PDF fits with varying jet input data [23].

#### 3.2 $W^\pm$ Charge Asymmetry

At the Tevatron  $W$  bosons are produced mainly from a quark of the proton and an anti-quark of the anti-proton. On average the  $u$ -quark momentum fraction is larger than the  $d$ -quark. Therefore the  $W^+$  ( $W^-$ ) is preferentially boosted along the (anti-)proton direction. Both experiments presented measurements of the  $W^\pm$  charge asymmetry measurement based on their Tevatron Run II data using the standard approach which relies on the rapidity of the  $W$  decay lepton. CDF also employs a method which directly reconstructs the  $W^\pm$  rapidity with up to two-fold ambiguity based on the  $W$  mass as a constraint [21]. Results from both experiments are shown in Fig. 7. The uncertainties of the measurements using  $1 \text{ fb}^{-1}$

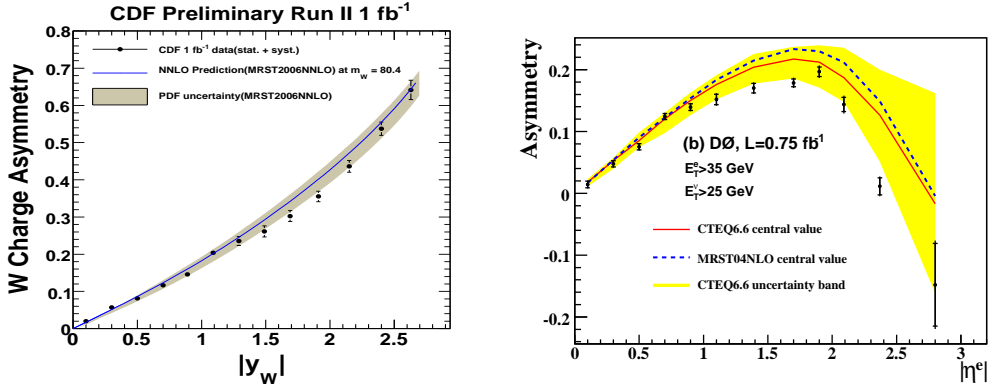


Figure 7: Measurements of the  $W^\pm$  charge asymmetry as a function of rapidity of the  $W$  boson (CDF, left) and of  $W$  decay lepton (right,  $D\phi$ ).

(CDF) and  $0.76 \text{ fb}^{-1}$  ( $D\phi$ ) are smaller than the uncertainty attributed to the PDFs in the prediction, indicating the constraining power of this type of measurement.

### 3.3 $Z$ Boson Production

At the Tevatron  $Z$  bosons are produced via quark anti-quark annihilation. The  $Z$  boson rapidity is directly related to the momentum fractions of the incoming partons of the hard interaction process. CDF presented measurement of the  $\gamma^*/Z$  production cross section, which extends to a boson rapidity of  $y = 3$ . This new measurement, shown in Fig. 8, is based on  $2.1 \text{ fb}^{-1}$ .  $D\phi$  presented measurements of the  $Z$  production cross section as a function of the transverse momentum of the  $Z$ -boson.  $D\phi$  also presented a measurement of the  $Z$  forward backward asymmetry,  $A_{FB}$  based on  $1.1 \text{ fb}^{-1}$ . At present the precision is still statistically limited, however in future, with 6 to  $8 \text{ fb}^{-1}$  anticipated for the Tevatron Run II, the measurement of  $A_{FB}$  is expected to provide further constraints on PDFs.

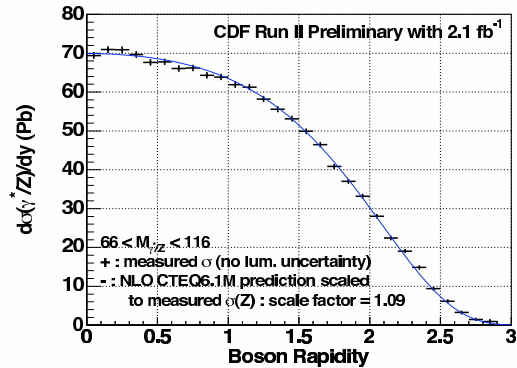


Figure 8: Rapidity distribution of  $Z$  bosons measured by CDF compared to perturbative QCD predictions at NLO.

## 4 Extraction of Parton Densities

Progress in obtaining an improved quantitative understanding of parton distribution functions and their uncertainties was reported at the meeting.

### 4.1 Extractions of PDFs at HERA

In both collaborations, H1 and ZEUS, the extraction of PDFs is an very active field of investigation. Naturally activities in both collaborations are focusing on the HERA data.

Cooper-Sakar presented a preliminary PDF analysis in the spirit of the ZEUS-JETS fit [10] which incorporates the new ZEUS measurements of NC and CC cross sections at high  $Q^2$  as well as the high  $y$  cross sections made available together with the measurement of  $F_L$ , see above. While the high- $Q^2$  data sets reduce the uncertainty of the valence quarks at high  $x$ , the medium- $Q^2$  high- $y$  data impact the gluon and sea quark distributions.

A new PDF fit to H1 data alone, labelled H1PDF2009 [2], was presented by Kretzschmar. Radescu discussed the update of the PDF fit to the HERA combined cross sections, labelled HERAPDF0.2. In both studies incorporating the new more precise measurements reduces the experimental uncertainties of the extracted PDFs to a level that model and parameterisation uncertainties become more important. In addition to the model uncertainties already considered in the earlier studies (H1PDF2000 [11] and HERAPDF0.1 [22]) the parameterisation uncertainty is estimated by calculating the envelope of PDF error bands obtained from fits of compatible quality with additional terms in the PDF parameterisations.

### 4.2 Global PDF Fits

In the context of best global fits Thorne reported on the recently published MSTW08 NLO DGLAP global fit [23]. The main new ingredients to the fit are NuTeV and CCFR dimuon data, constraining the strange sea, inclusive jet data from HERA and the Tevatron, lepton asymmetry data and Z-boson rapidity measurements from CDF and  $D\bar{O}$  and all at the time of publication available charm structure function data. Considerable work went into the procedure to evaluate the PDF uncertainties by applying a more sophisticated tolerance criterion to deal with tensions between the input datasets.

Recent work of the CTEQ collaboration towards a new set of PDFs, CT09 [24], was reviewed by Nadolsky and Lai. The new analysis incorporates a variety of measurements from Tevatron with sensitivity to PDF, see above. The impact of the Tevatron Run-II jet data on the gluon distribution was studied in great detail including an critical review of jet cross section predictions which were found to be satisfactory (although not perfect) at next to leading order. The compatibility of various data sets and sophisticated procedures to evaluate the PDF uncertainties are an active field of investigation.

Ubiali reported on the progress of the NNPDF collaboration towards a global PDF analysis [25]. Instead of parameterising the fitted PDFs with an arbitrarily chosen functional form this analysis employs neural networks, trained on Monte Carlo generated replica of the input data, to obtain a set of PDFs with an faithful estimate of the uncertainties [26]. A first set of PDFs from a comprehensive analysis of DIS data is now available, labelled NNPDF1.0. Work on including data from hadron hadron collisions is progressing, detailed comparisons to the H1 and MSTW fit look very promising. A parton set from the NNPDF collaboration, which can compete with the global analyses by CTEQ and MSTW, appears to be feasible in the near future.

### 4.3 Dedicated PDF Studies

Alekhin [27] and Rojo [28] presented detailed studies of the strange sea. These studies are motivated by the necessity of a flavour decomposition of the sea quarks to achieve a faithful estimate of the sea quark uncertainties. In addition an asymmetric strange sea might well explain the NuTeV anomaly [29]. Furthermore the strange quark contribution to the W-production at the LHC is of the same order of magnitude as the non-strange contribution. These analyses include the (anti)neutrino data by the CCFR and NuTeV collaborations in a global NLO fit to inclusive charged lepton-nucleon DIS and Drell-Yan data. A strange sea suppression factor  $\kappa = \int_0^1 x[s(x) + \bar{s}(x)]dx / \int_0^1 x[\bar{u}(x) + \bar{d}(x)]dx$  of  $0.62 \pm 0.04(\text{exp}) \pm 0.03(\text{QCD})$  at  $Q^2 = 20 \text{ GeV}^2$  is obtained and the strange sea is found to be slightly softer than the non-strange sea. The  $x(s - \bar{s})$  asymmetry is compatible with zero within errors, as can be seen in Fig. 9. The asymmetry changes sign when only including either CCFR or NuTeV data and is also sensitive to nuclear and higher order QCD corrections.

An extraction of PDFs at high- $x$  [30], a study performed in close collaboration with the CTEQ collaboration, was presented by Keppel. The goal of this study is to extend the standard CTEQ global PDF fit to larger values of  $x$  and lower values of  $Q^2$ , taking advantage of a host of new results from Jefferson Lab experiments, as well as COMPASS and HERMES, which provide valuable high precision inputs in the high- $x$  region. Preliminary results of this study indicate that extracted PDFs are relatively insensitive to higher twist and target mass corrections as long as these corrections are simultaneously taken into account. The reduction of the PDF uncertainty at high  $x$  in this preliminary study is quite encouraging. The indication of  $d$ -quark suppression at high  $x$  is an intriguing suggestion. Precise PDFs at high- $x$  are and will be an important input to current and upcoming neutrino oscillation experiments, and could also prove to be relevant for heavy particle production at the hadron colliders Tevatron and LHC.

The extraction of nuclear PDFs [31], presented by Paukkunen, aims for a process independent nuclear PDF-set. The difference of free versus bound nucleons is taken into account by defining the bound proton PDFs in a nucleons of nucleon number  $A$  relative to the free PDF as  $f_i^A(x, Q^2) \equiv R_i^A(x, Q^2) f_i^{\text{CTEQ6.1M}}(x, Q^2)$ . An excellent agreement between NLO pQCD and the hard process nuclear data for DIS, Drell-Yan and  $\pi^0$  production over a wide kinematic range of  $0.005 < x < 1$  and  $1.69 < Q^2 < 150 \text{ GeV}^2$  is found, leading to the conclusion that the factorisation theorem in hard nuclear scattering processes works well. Further experiments, e.g. proton-ion collisions at the LHC or electron-ion colliders such as eRHIC and LHeC may be needed to find possible violations of the factorisation theorem.

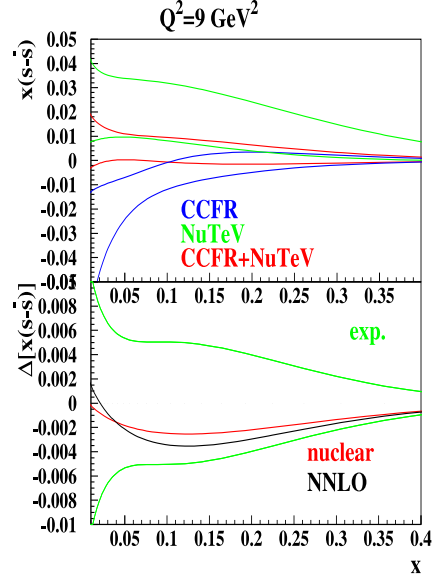


Figure 9: The strange sea asymmetry (top and its uncertainty (bottom) in various fit scenarios.



## 5 Outlook on LHC

The LHC start-up will bring particle physics to a new energy regime. The ATLAS, CMS and LHCb experiments are eagerly awaiting first data. The first challenge will be to “rediscover” the Standard Model at the LHC energy scale. Measuring the production of the  $W$  and  $Z$  bosons will be an important milestone, which will test the understanding of the detector calibrations as well as our knowledge of the Standard Model.

The uncertainties of the PDFs constitute the main source of theory uncertainty. Measurements of the rapidity distribution of the  $W$ -decay leptons and the  $W$ -asymmetry in the early data of  $100\text{pb}^{-1}$  have the potential to improve our knowledge of PDFs, if the experimental systematics can be controlled with a precision better than 5%. With increasing integrated luminosity a fit to the  $Z$  and  $W$  rapidity distributions should allow to measure the luminosity in the LHCb interaction region with a precision of one to two percent. A study of Drell-Yan events shows that LHCb has the capability to trigger and reconstruct Drell-Yan muon-pairs at a mass  $M(\mu\mu) > 2.5\text{GeV}^2$ . These events probe  $x$ -values down to  $1.5 \cdot 10^{-6}$ , i.e.  $x$  values probed at HERA only at low values and limited range in  $Q^2$ . Therefore the measurement could provide an important test of the extrapolation of PDFs to much higher scales.

For further details of the LHC related studies presented by Anderson, Cepeda and De Lorenzi, see their contributions in these proceedings.

## 6 Theoretical Developments

The theoretical talks in this working group can be naturally divided into two categories: those describing general aspects of structure functions and those focused on phenomena at low values of Bjorken  $x$ . In the former there were five contributions and in the latter eleven. We make a short description of each of them in the following two subsections.

### 6.1 Structure Functions

There were three contributions devoted to the investigation of the higher-loop structure of Feynman diagrams.

Jos Vermaseren explained in detail what are the main obstacles when calculating structure functions at higher orders in the strong coupling. The natural space for these complicated calculations is the Mellin representation, this brings harmonic sums into the game. The inversion of these sum has as a consequence the appearance of harmonic polylogarithms. Many times these new functions arise after the application of a Mellin-Barnes technique which has the advantage of making the Lorenz integrations rather straightforward. Relations among the different harmonic polylogarithms allow for simplification of initially very complicated expressions. Of particular importance are the Multiple Zeta Values (MZV's) which are related to infinite sums of harmonic sums. To reduce them into a simple basis is a formidable task which has been at the hands of mathematicians from the 90's, useful tricks are the so-called 'shuffle' and 'stuffle' algebras. An important tool provided by Vermaseren and collaborators for the reduction of expressions is the code named as TFORM. He showed tables for the MZV's which cover all cases up to 6-loop coefficient functions. In Ref. [32] further details can be found.

Advanced reduction techniques using computers were also shown by Johannes Blümlein for the calculation of 3-loop anomalous dimensions and Wilson coefficients. He explained that single scale quantities depending on a ratio of Lorentz invariants can be transformed into a Mellin representation, when the Mellin-conjugate variable of this ratio is considered as discrete we can describe the calculation in terms of difference equations. In this way one can reconstruct the general formula up to 3-loop order for single scale quantities out of a finite number of fixed moments. This task is facilitated by the recurrence relations polynomials and nested harmonic sums fulfil. To solve the difference equation order by order they use the package “sigma”. The main reference is Ref. [33].

New higher-order results for 3-loop coefficient function of the structure function  $F_3^{\nu+\bar{\nu}}$  were also discussed by Andreas Vogt. He remarked the appearance of new colour structures proportional to the  $d^{abc}d_{abc}$  group invariant which are suppressed at  $x \rightarrow 1$  but have a large effect at small  $x$ . For the coefficient functions for  $F_L$  he remarked the very slow convergence of the perturbative expansion. See Ref. [34, 35] for more details.

A global analysis of parton distribution functions including a  $p_T$  resummation was discussed by Hung-Liang Lai [36]. In this presentation the importance of the high precision measurement of the  $W$  mass, as well as its  $Q_T$  (due to the recoil of the  $W$  in the transverse plane), was emphasised. A transverse momentum resummation of the leading logarithms generating the latter quantity was performed using the Collins-Soper-Sterman formalism. This also included some treatment of the non-perturbative higher twist effects. In the combined PDF and  $p_T$  global analysis as new inputs they also included the  $p_T$  of Drell-Yan pairs and  $Z$  bosons.

A description of  $F_L$  within the context of a colour-dipole model was provided by Dieter Schildknecht. He made an introduction to DIS at low  $x$  from the point of view of colour-dipole interactions remarking the difference in the transverse momentum of  $q\bar{q}$  pairs when produced from longitudinal or transverse virtual photons. As a consequence, the interesting relation  $F_L = 0.27F_2$  was derived with a minimal set of assumptions in their model. A description of geometric scaling was also provided.

## 6.2 Low- $x$

There were many talks and hot discussions in the low  $x$  sessions. Felipe Llanes-Estrada described what he considered a loophole in the Deeply Virtual Compton Scattering (DVCS) factorisation theorems. For this they assumed, in the quark-nucleon scattering amplitude, a Regge behaviour independent of the number of quarks. This leads to a similar Regge form in structure functions and leads to a breakdown of the collinear factorisation in DVCS. The interested reader can consult Ref. [37].

The difficult problem of a consistent treatment of unitarity corrections was addressed by Gian Paolo Vacca. If one wants to attack this problem using reggeized gluons as the correct degrees of freedom then it is very complicated since these are non local composite states. One can use a simplified effective field theory introduced by Gribov in the times before QCD. In this case the problem is reduced to zero transverse dimensions and is equivalent to a quantum mechanics of locally interacting pomerons. The model proposed by Vacca allows for the inclusion of pomeron loops induced by interactions. The relevant references are [38, 39].

Many talks of phenomenological nature were focused on the application of evolution equations including DGLAP and BFKL type of resummations to the description of  $F_{2,L}$ .

This is the case of the contribution of Anna Staśto where she considers a DGLAP/BFKL unified approach to make predictions for  $F_L$ . The BFKL kernel is supplemented by a kinematic constraint, DGLAP splitting functions are included and running coupling effects taken into account. In this way both the collinear and dipole model limits are correctly obtained. Good agreement with HERA data was found and predictions for the LHeC were given, as can be found in Ref. [40].

In a similar spirit Henri Kowalski explained an interesting calculation of the gluon density at small  $x$  using the BFKL equation modified in the infrared and improved by collinear effects. Their matching between the perturbative and non-perturbative regions discretizes the eigenfunctions of the kernel when the running of the coupling is considered, introducing phases which carry non-perturbative information. Playing with their values they managed to get accurate phenomenology for HERA data, see Ref. [41].

The renormalisation group improved BFKL equation underlies many of the different approaches presented in our working group. A very detailed description of it was given by Dimitri Colferai [42]. He went into the technicalities of consistently including quarks into the game using a matrix form within a collinear factorisation scheme very close to  $\overline{\text{MS}}$  since the anomalous dimensions in this scheme are incorporated up to NLO. In the gluon channel the NLL BFKL kernel is included. Results for the resummed splitting function matrix were shown.

An alternative to the RG-improved kernels just summarised is that of exploiting the existing duality between the DGLAP and the BFKL approaches in the fixed coupling limit. The phenomenological implications of this idea were highlighted by Juan Rojo [43]. The resummed  $P_{gg}$  is very similar to that presented by Colferai and a smooth large  $Q^2$  limit for  $K$  factors is achieved. Results for  $F_L$  and predictions for LHeC were also explained.

The application of high energy resummations in Drell-Yan production was discussed by Simone Marzani. He explained how this cross section is one of the better known at the LHC and how it can be complemented by a small  $x$  resummation in the large rapidity region. The calculation now requires the sum to the fixed order coefficient function of a tower of small  $x$  logarithms and of subtraction terms to avoid double counting. All of this is performed in terms of Mellin moments. At NLO the small  $x$  corrections are of the order of a 5 to 10 percent, see Ref. [44, 45]. These effects will be more sizable in rapidity distributions.

As part of a joint session together with the Diffraction and Vector Mesons working group, Javier Albacete presented a global analysis of DIS inclusive structure function data using the BK equation [46, 47, 48]. They used a form of running the coupling based on a ratio of coupling functions at different scales related to the dipole size. As usual, the effect of the running is to reduce the onset of small  $x$  corrections making the predictions more compatible with the experimental data. They also obtained a good fit of  $F_L$  and made predictions for the LHeC.

An interesting talk by Emil Avsar was based on how to introduce an absorptive barrier in order to impose unitarity constraints in the CCFM equation, whose physical principle for resummation is angular ordering. This opens up the possibility to study unitarity effects in exclusive observable, an important road since it is very difficult to discriminate among different evolution approaches using only inclusive distributions. His approach is very flexible since it is already implemented in a Monte Carlo. Ref. [49, 50] contains all the details.

Finally, it was a great pleasure to attend the two more formal contributions of our working group related to the structure of the NLO corrections to the BK and BFKL equations, presented by Victor Fadin and Ian Balitsky. Fadin over-viewed the ambiguities present at

NLO in the BFKL calculation. To be aware of the freedom in the definition of the formalism allows for a correct investigation of its conformal properties in the two dimensional transverse space. The game in the last few years has been to compare the original BFKL approach, based on the gluon Reggeization and bootstrap consistency conditions, with the colour dipole picture [51]. The mapping between both is simple at LO but more complicated at NLO, however, taking into account the definition of the impact factors and the choice of the energy scale present in the logarithms of energy, it is possible to show that both approaches give equivalent evolution equations.

The description of high energy scattering in terms of Wilson lines discussed by Balitsky is always very appealing. This allows for a direct calculation of evolution kernels in terms of colour dipoles propagating in the background of colour shock waves. Here the nonlinearity of the dipole evolution is immediately manifest. Recently the NLO corrections to the BK equation have been obtained, and can be found in Ref. [52].

## Acknowledgement

We very much enjoyed this well organised workshop in the beautiful town of Madrid, and we thank the local organisers for their support and hospitality extended to us. We would also like to thank all those who contributed to the structure function session either by preparing talks or by taking part in the lively discussions.

## References

- [1] Slides:  
<http://indico.cern.ch/contributionDisplay.py?contribId=326&sessionId=22&confId=53294>  
<http://indico.cern.ch/contributionDisplay.py?contribId=15&sessionId=22&confId=53294>
- [2] H1 Collaboration, F.D. Aaron *et al.*, submitted to Eur. Phys. J. C, arXiv:0904.3513 [hep-ex].
- [3] H1 Collaboration, F.D. Aaron *et al.*, submitted to Eur. Phys. J. C, arXiv:0904.0929 [hep-ex].
- [4] H1 Collaboration, C. Adloff *et al.*, Eur. Phys. J. **C21** 33 (2001) [arXiv:0012053 [hep-ex]],  
H1 Collaboration, C. Adloff *et al.*, Nucl. Phys. B 497, 3 (1997) [arXiv:9703012 [hep-ex]].
- [5] K. Golec-Biernat and M. Wüsthoff, Phys. Rev. **D59**, 014017 (1999) [arXiv:9807513 [hep-ph]].
- [6] E. Iancu, K. Itakura and S. Munier, Phys. Lett. **B590**, 199 (2004) [arXiv:0310338 [hep-ph]].
- [7] T. Laštovička, Eur. Phys. J. **C24**, 529 (2002) [arXiv:0203260 [hep-ph]].
- [8] H1 Collaboration, F.D. Aaron *et al.*, Phys. Lett. **B665**, 139 (2008) [arXiv:0805.2809 [hep-ex]].
- [9] ZEUS Collaboration, S. Chekanov *et al.*, submitted to Phys. Lett. B, arXiv:09041092 [hep-ex].
- [10] ZEUS Collaboration, S. Chekanov *et al.*, Eur. Phys. J. **bf C42**, 1 (2005) [arXiv:0503274 [hep-ph]].
- [11] H1 Collaboration, C. Adloff *et al.*, Eur. Phys. J. **C30**, 1 (2003) [arXiv:0304003 [hep-ex]].
- [12] ZEUS Collaboration, S. Chekanov *et al.*, accepted by Eur. Phys. J. C, arXiv:09012385 [hep-ex].
- [13] ZEUS Collaboration, S. Chekanov *et al.*, Eur. Phys. J. **C61** 223 (2009) [arXiv:08124620 [hep-ex]].
- [14] J. Feltesse, Proceedings of DIS 2008, doi:10.3360/dis.2008.24  
A. Glazov, AIP Conf. Proc. **792**, 237 (2005)
- [15] ZEUS Collaboration, J. Breitweg *et al.*, Phys. Lett. **B407**, 432 (1997), [arXiv:9707025 [hep-ex]].
- [16] ZEUS Collaboration, J. Breitweg *et al.*, Phys. Lett. **B487**, 53 (2000) [arXiv:0005018 [hep-ex]].
- [17] ZEUS Collaboration, J. Breitweg *et al.*, Eur. Phys. J. **C7**, 609 (1999) [arXiv:9809005 [hep-ex]].
- [18] CDF Collaboration, A. Abulencia *et al.*, Phys. Rev. **D75**, 092006 (2007),  
Erratum *ibid.* **D75**, 119901 (2007) [arXiv:0701051 [hep-ex]].

- [19] CDF Collaboration, A. Aaltonen *et al.*, Phys. Rev. **D78**, 052006 (2008),  
Erratum *ibid.* **D79**, 119902 (2009) [arXiv:0807.2204 [hep-ex]].
- [20] DØ Collaboration, V.M. Abazov *et al.*, Phys. Rev. Lett. **101**, 062001 (2008) [arXiv:0802.2400 [hep-ex]].
- [21] A. Bodek *et al.*, Phys. Rev. **D77**, 111301 (2008) [arXiv:07112859 [hep-ph]].
- [22] H1 and ZEUS Collaborations, H1prelim-09-045, ZEUS-prel-09-011.  
B. Reisert, Proceedings of the ICHEP 2008, arXiv:0809.4946 [hep-ex].
- [23] A.D. Martin *et al.*, Submitted to Eur. Phys. J. C, arXiv:0901.0002 [hep-ph].
- [24] J. Pumplin *et al.*, Phys. Rev. **D80**, 014019 (2009), see also arXiv:0904.2424 [hep-ph]
- [25] NNPDF Collaboration, R.D. Ball *et al.*, Nucl. Phys. **B809**, 1 (2009), arXiv:0808.1231 [hep-ph], and  
references therein.
- [26] M. Ubiali, Nucl. Phys. Proc. Suppl. **186**, 62 (2009) [arXiv:0809.3716 [hep-ph]].
- [27] S. Alekhin *et al.*, Phys. Lett. **B675**, 433 (2009) [arXiv:0812.4448 [hep-ph]].
- [28] NNPDF Collaboration, R.D. Ball *et al.*, arXiv:09061958 [hep-ph].
- [29] S. Davidson *et al.*, JHEP **0202**, 037 (2002) [arXiv:0112302 [hep-ph]].
- [30] J.F. Owens *et al.*, Phys. Rev. **D75**, 054030 [arXiv:0702159 [hep-ph]].
- [31] K.J. Eskola *et al.*, JHEP **0904**, 065 (2009) [arXiv:09024154 [hep-ph]].
- [32] J. Blümlein, D. J. Broadhurst and J. A. M. Vermaseren, arXiv:0907.2557 [math-ph].
- [33] J. Blümlein, M. Kauer, S. Klein and C. Schneider, arXiv:0902.4091 [hep-ph].
- [34] S. Moch, J. A. M. Vermaseren and A. Vogt, arXiv:0812.4168 [hep-ph].
- [35] S. Moch and A. Vogt, JHEP **0904** (2009) 081 [arXiv:0902.2342 [hep-ph]].
- [36] P. M. Nadolsky *et al.*, Phys. Rev. D **78** (2008) 013004 [arXiv:0802.0007 [hep-ph]].
- [37] S. J. Brodsky, F. J. Llanes-Estrada, J. T. Londergan and A. P. Szczepaniak, arXiv:0906.5515 [hep-ph].
- [38] M. A. Braun and G. P. Vacca, Eur. Phys. J. C **50** (2007) 857 [arXiv:hep-ph/0612162].
- [39] G. P. Vacca, arXiv:0907.2581 [hep-ph].
- [40] K. Golec-Biernat and A. M. Stasto, Phys. Rev. D **80** (2009) 014006 [arXiv:0905.1321 [hep-ph]].
- [41] J. Ellis, H. Kowalski and D. A. Ross, Phys. Lett. B **668** (2008) 51 [arXiv:0803.0258 [hep-ph]].
- [42] M. Ciafaloni, D. Colferai, G. P. Salam and A. M. Stasto, JHEP **0708** (2007) 046 [arXiv:0707.1453  
[hep-ph]].
- [43] J. Rojo, G. Altarelli, R. D. Ball and S. Forte, arXiv:0907.0443 [hep-ph].
- [44] S. Marzani and R. D. Ball, Nucl. Phys. B **814** (2009) 246 [arXiv:0812.3602 [hep-ph]].
- [45] S. Marzani and R. D. Ball, arXiv:0906.4729 [hep-ph].
- [46] J. L. Albacete and Y. V. Kovchegov, Phys. Rev. D **75** (2007) 125021 [arXiv:0704.0612 [hep-ph]].
- [47] J. L. Albacete, Phys. Rev. Lett. **99** (2007) 262301 [arXiv:0707.2545 [hep-ph]].
- [48] J. L. Albacete, N. Armesto, J. G. Milhano and C. A. Salgado, arXiv:0902.1112 [hep-ph].
- [49] E. Avsar and E. Iancu, Phys. Lett. B **673** (2009) 24 [arXiv:0901.2873 [hep-ph]].
- [50] E. Avsar and E. Iancu, arXiv:0906.2683 [hep-ph].
- [51] V. S. Fadin, R. Fiore and A. V. Grabovsky, Nucl. Phys. B **820** (2009) 334 [arXiv:0904.0702 [hep-ph]].
- [52] I. Balitsky and G. A. Chirilli, Phys. Rev. D **77** (2008) 014019 [arXiv:0710.4330 [hep-ph]].